

Marshall University
Marshall Digital Scholar

Physics Faculty Research

Physics

1-1-2007

Contact printed Co/insulator/Co molecular junctions

Xiaojuan Fan

Marshall University, fan2@marshall.edu

David L. Rogow

Claudia H. Swanson

Akhilesh Tripathi

Scott R. J. Oliver

Follow this and additional works at: http://mds.marshall.edu/physics_faculty

 Part of the [Physics Commons](#)

Recommended Citation

Fan, X., Rogow, D. L., Swanson, C. H., Tripathi, A., & Oliver, S. R. (2007). Contact printed Co/insulator/Co molecular junctions. *Applied Physics Letters*, 90(16):163114.

This Article is brought to you for free and open access by the Physics at Marshall Digital Scholar. It has been accepted for inclusion in Physics Faculty Research by an authorized administrator of Marshall Digital Scholar. For more information, please contact zhangj@marshall.edu.

Contact printed Co/insulator/Co molecular junctions

Xiaojuan Fan, David L. Rogow, and Claudia H. Swanson

Department of Chemistry and Biochemistry, University of California, Santa Cruz, California 95064

Akhilesh Tripathi

Rigaku Americas Corporation, 9009 New Trails Drive, The Woodlands, Texas 77381

Scott R. J. Oliver^{a)}

Department of Chemistry and Biochemistry, University of California, Santa Cruz, California 95064

(Received 13 March 2007; accepted 19 March 2007; published online 19 April 2007)

The authors report the contact printing of a Au/Co double layer (total thickness $\sim 20\text{--}40$ nm) onto a self-assembled monolayer surface to form molecular junctions under ambient conditions. The feature size ranges from $50 \times 50 \mu\text{m}^2$ to $2 \times 2 \text{mm}^2$. Grazing incident x-ray diffraction of the multilayer junction shows all expected Au peaks, while elemental Co was confirmed by energy dispersive spectroscopy. Film thickness, roughness, and density were characterized by x-ray reflectivity. *I-V* measurements show a prominent hysteresis, likely associated with charge trapping at the metal-organic interface, not an intrinsic feature of alkanedithiol molecules. © 2007 American Institute of Physics. [DOI: 10.1063/1.2728741]

Growing efforts have been dedicated to organic monolayer junctions that may afford a new generation of devices of far smaller size and higher density. The most common arrangement simply consists of two metal electrodes in direct contact with molecules that fingerprint their current-voltage response. Various architectures of molecular junctions have been reported, including mercury drop,¹ nanopore,² cold break,³ cross-wire,^{4,5} and scanning probe microscopy tip-based junctions.^{6,7} Observed transport behaviors for these junctions include negative differential resistance,⁸ rectification,⁹ quantum conductance,¹⁰ and two-state switching.¹¹ These phenomena are attributed to molecular tilt,¹² asymmetric electrode coupling,¹³ metal work function,¹⁴ and interfacial dipole moment.¹⁵

Among the different types of molecular junction architectures, planar junctions are the most compatible with creating large size features up to millimeters. Large-area molecular devices are typically required for spectroscopic analysis, such as Raman scattering, optical, and x-ray photoelectron spectroscopy. The main challenge in their fabrication remains to be the deposition of a top metal contact onto the organic molecular surface. For any conventional metal deposition method such as evaporation or sputtering, the process easily decomposes the underlying molecular layer, creating metallic shorting.¹⁶ Recent efforts have focused on indirect evaporations such as soft lithography,¹⁷ nanotransfer printing,¹⁸ and lift-off processes.¹⁹ Contact printing is one of the most promising alternatives for depositing the top metal electrode without degradation of the underlying self-assembled monolayer (SAM).^{18,20,21} Thus far, contact printing has been only applied to noble metals such as Au, Ag, and Pt.^{22,23} We report here large-area metal/SAM/metal junctions based on magnetic metal cobalt, created by coupling the techniques of self-assembly and contact printing.

The Au/Co/SAM/Co/Au junction array was patterned on a Si wafer. The bottom metal electrode (8 nm Ti adhesion layer, followed by 100 nm Au and 40 nm Co) was deposited sequentially by e-beam evaporation on the Si substrate. A

dithiol SAM was then formed on the Co film by immersing the substrate in a 10 mM methyl ethyl ketone (MEK) solution of 1,10-decanedithiol [$\text{HS}(\text{CH}_2)_{10}\text{SH}$] for 24 h. The monolayer-coated samples were removed from solution, rinsed with MEK, and dried in a stream of N_2 gas.

Detailed fabrication procedures for the photoresist negative mold and poly(dimethylsiloxane) (PDMS) stamp can be found elsewhere.²⁴ The bare PDMS stamp was placed in the e-beam evaporator and coated with a metal bilayer film (20 nm Au followed by 20 nm Co, such that Co is the exposed top layer, and subsequently Au after contact printing). The stamp was then immediately placed onto the SAM surface for several seconds without extra manual pressure. Peeling away the stamp left the metal film on the SAM surface and completed the junction fabrication.

Grazing incident x-ray diffraction (GIXRD) data were collected with a 0.04° step size, 1 s step time, and $10^\circ\text{--}80^\circ$ 2θ scan range. Film thickness, density, and surface/interface roughness were determined by x-ray reflectivity (XRR) data and analysis. The *I-V* measurements were performed under ambient conditions with a picoammeter under computer control.

The Au/Co/SAM/Co/Au junction feature size ranged from $50 \times 50 \mu\text{m}^2$ to $2 \times 2 \text{mm}^2$. The lower size limit is $1 \times 1 \mu\text{m}^2$, that of the conventional lithography used. Cobalt sandwiches the alkanedithiol monolayer on both sides [Fig. 1(a)]. The Au metal is used to facilitate contact printing transfer, as well as to help protect Co from oxidation. Interfacial electronic studies by Caruso *et al.* of thiol terminated SAMs on Co and Au surfaces suggest that thiols bond to cobalt surfaces stronger compared to gold surfaces.²⁵ Figure 1(a) is a schematic illustration of both the molecular junction array and electrical circuit used for *I-V* measurement. Figure 1(b) is an optical reflectance micrograph of the Au/Co/SAM/Co/Au junction array. The square size in this example is $\sim 50 \times 50 \mu\text{m}^2$. The darker color regions are metal printed from the PDMS stamp, while the lighter color circular regions are uncoated bare substrate-metal-SAM areas surrounding the squares. This phenomenon is due to stamp deformation during contact printing, as we recently

^{a)}Electronic mail: soliver@chemistry.ucsc.edu

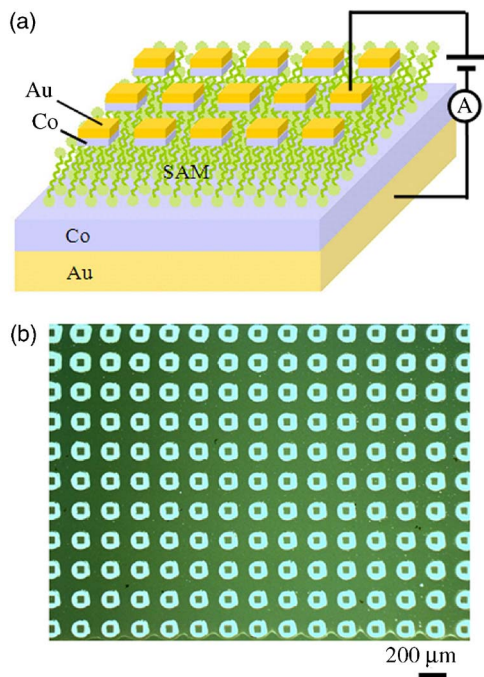


FIG. 1. (Color online) (a) Schematic of the molecular sandwich array and the two-terminal electrical transport circuit. (b) Micrograph of a Au/Co/SAM/Co/Au junction array. Dark areas are printed metal bilayer; light circular areas around the square features are areas where no printing occurred due to deformation of the stamp during contact.

described in detail for Ag-based films.²⁴ The patterned junctions were created in parallel without chemical-based etching steps, enabling a rapid fabrication of thousands of devices on a single wafer in a single step.

The GIXRD pattern of the multilayered film is shown in Fig. 2. All expected polycrystalline Au peaks are present in the diffraction pattern. No Co peaks are observed, possibly due to its x-ray amorphous nature.²⁶ XRR data are presented in Fig. 3, and the resultant density, surface roughness, and thickness of each layer are summarized in Table I. The experimental SAM thickness is ~ 1.31 nm, indicating that the decanedithiol molecules (molecular length ~ 1.45 nm, from the Cambridge Structural Database) are tilted with respect to the surface normal by $\sim 33^\circ$, in close agreement with the theoretical and experimental value of 30° .²⁷ The top Co layer

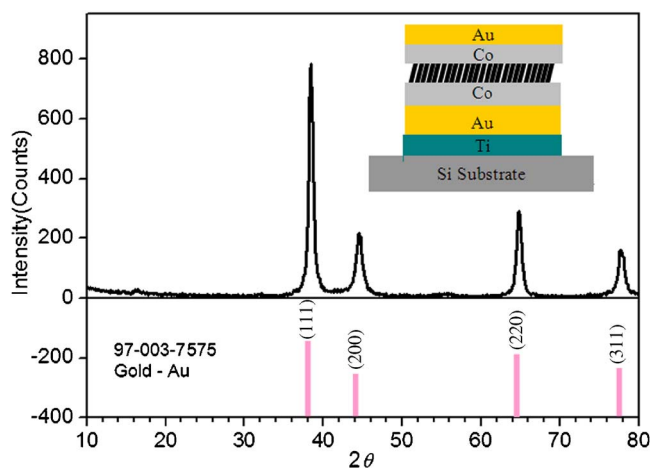


FIG. 2. (Color online) GIXRD pattern of the Au/Co/SAM/Co/Au array shows all expected Au peaks. The absence of Co peaks is likely due to its x-ray amorphous nature.

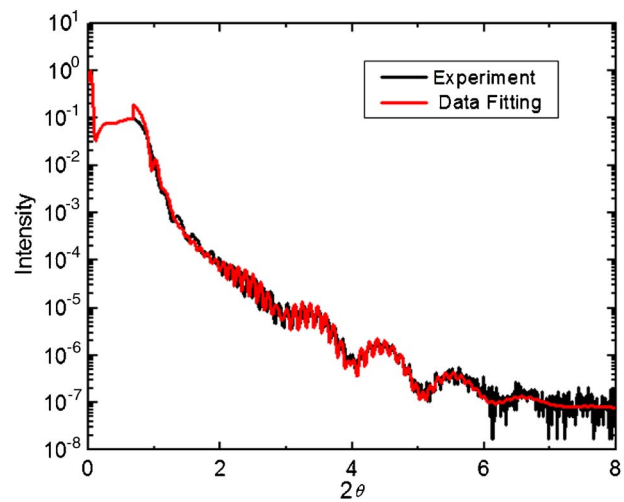


FIG. 3. (Color online) X-ray reflectivity measurement (black line) and data fitting (red line) yield the parameters shown in Table I.

thickness of ~ 21 nm is very close to the expected value of 20 nm. The top Au layer (thickness ~ 8 nm) has an experimental density of ~ 14.50 g/cm³, lower than the standard value for bulk Au of 19.30 g/cm³. In contrast, the much thicker bottom Au layer has an XRR density of 19.33 g/cm³, almost the same as the standard value for bulk Au, indicating that the layer is more condensed. The top Co layer shows a density of 9.53 g/cm³, very close to that of bulk Co, 8.90 g/cm³.

The roughness of the bottom double layer is 1.461 nm, much less than that of the top Au and Co layers, 3.988 and 4.396 nm, respectively. This observation is not surprising since the bottom metal bilayer was e-beam evaporated directly on the polished single crystalline Si substrate, while the top bilayer was contact printed from the PDMS stamp surface and likely involved some degree of recrystallization.²⁸ Energy dispersive spectroscopy of the printed area gave all expected elemental peaks of Au and Co (not shown), confirming the existence of Co despite the lack of peaks in the GIXRD pattern.

Two-terminal transport measurements were performed on the junctions. Figure 4 shows a typical two-probe I - V curve from the setup depicted in Fig. 1(a). As expected, the resistance of the SAM junction was significantly high, $\sim 1.2 \times 10^{10}$ Ω (obtained from curve 1 in the low bias region of 0–0.3 V, Fig. 4). This value agrees well with literature values for alkanedithiol SAMs, in the range of 10^6 – 10^{12} Ω .^{14,29} Arrows and numbers indicate the voltage sweeping directions. From 0 to 1 V (curve 1), the current shows a linear relation up to ~ 0.3 V, then deviates from linearity. This nonlinear feature at relatively large bias is

TABLE I. Film thickness, roughness, and density derived from XRR data.

No.	Name	Density (g/cm ³)	Thickness (nm)	Roughness (nm)
5	Au	14.548 92	8.032	3.988
4	Co	8.625 75	21.313	4.396
3	C ₁₀ H ₂₂ S ₂	1.009 50	1.315	0.537
2	Co/Au	19.326 35	67.979	1.461
1	Ti	9.527 13	7.986	0.405
0	Si	2.330 00	0.000	0.364

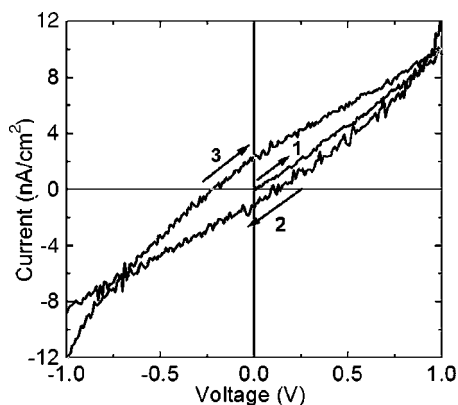


FIG. 4. Current-voltage curve of the molecular junction; arrows represent the voltage sweeping direction and order.

typical for current tunneling through organic molecular layers.^{1,4–6,30,31} The current then shows a hysteresis when the applied voltage is swept between 1.0 and -1.0 V.

No such behavior is observed for previously published alkanethiol or alkanedithiol SAM junctions using Au, Ag, or Pt metal electrodes.^{4,14,31,32} Recently, however, hysteresis has been reported in various molecular junctions regardless of the junction configuration, such as controllable switching in an eicosanoic acid crossbar junction device.^{33–35} Charge trapping by defects located at the molecule-metal interface accounted for the switching hysteresis of the planar crossbar device. The prominent hysteresis in our samples is therefore most likely due to charge trapping at the interfaces of Co and alkanedithiol molecules. We are currently studying related systems with other magnetic metals for further investigation of this hysteresis.

In summary, we have created metal/SAM/metal molecular junctions involving magnetic metal Co, deposited by contact printing without the need for costly fabrication equipment. XRD and XRR show expected film structures, roughness, density, and thickness. Current-voltage hysteresis is attributed to charge trapping effects at the interface of cobalt and SAM. Co metal in a molecular junction may be particularly valuable in spintronic applications.

This work was performed in part at the Stanford Nanofabrication Facility of NNIN supported by the National Science Foundation under Grant ECS-9731293.

¹R. E. Holmlin, R. Haag, M. L. Chabinyc, R. F. Ismagilov, A. E. Cohen, A. Terfort, M. A. Rampi, and G. M. Whitesides, *J. Am. Chem. Soc.* **123**, 5075 (2001).

²W. Y. Wang, T. Lee, and M. A. Reed, *Phys. Rev. B* **68**, 035416 (2003).

³J. Park, A. N. Pasupathy, J. I. Goldsmith, C. Chang, Y. Yaish, J. R. Petta, M. Rinkoski, J. P. Sethna, H. D. Abruna, P. L. McEuen, and D. C. Ralph, *Nature (London)* **417**, 722 (2002).

⁴M. A. Reed, C. Zhou, C. J. Muller, T. P. Burgin, and J. M. Tour, *Science* **278**, 252 (1997).

⁵A. S. Blum, J. G. Kushmerick, D. P. Long, C. H. Patterson, J. C. Yang,

J. C. Henderson, Y. X. Yao, J. M. Tour, R. Shashidhar, and B. R. Ratna, *Nat. Mater.* **4**, 167 (2005).

⁶X. D. Cui, X. Zaraté, J. Tomfohr, O. F. Sankey, A. Primak, A. L. Moore, T. A. Moore, D. Gust, G. Harris, and S. M. Lindsay, *Nanotechnology* **13**, 5 (2002).

⁷F. R. F. Fan, Y. X. Yao, L. T. Cai, L. Cheng, J. M. Tour, and A. J. Bard, *J. Am. Chem. Soc.* **126**, 4035 (2004).

⁸J. Chen, M. A. Reed, A. M. Rawlett, and J. M. Tour, *Science* **286**, 1550 (1999).

⁹C. Zhou, M. R. Deshpande, M. A. Reed, L. JonesII, and J. M. Tour, *Appl. Phys. Lett.* **71**, 2857 (1997).

¹⁰X. D. Cui, A. Primak, X. Zaraté, J. Tomfohr, O. F. Sankey, A. L. Moore, T. A. Moore, D. Gust, L. A. Nagahara, and S. M. Lindsay, *J. Phys. Chem. B* **106**, 8609 (2002).

¹¹C. N. Lau, D. R. Stewart, R. S. Williams, and M. Bockrath, *Nano Lett.* **4**, 569 (2004).

¹²Z. J. Donhauser, B. A. Mantooth, K. F. Kelly, L. A. Bumm, J. D. Monnell, J. J. Stapleton, D. W. Price, A. M. Rawlett, D. L. Allara, J. M. Tour, and P. S. Weiss, *Science* **292**, 2303 (2001).

¹³J. Taylor, M. Brandbyge, and K. Stokbro, *Phys. Rev. Lett.* **89**, 138301 (2002).

¹⁴V. B. Engelkes, J. M. Beebe, and C. D. Frisbie, *J. Am. Chem. Soc.* **126**, 14287 (2004).

¹⁵A. Vilan, J. Ghabboun, and D. Cahen, *J. Phys. Chem. B* **107**, 6360 (2003).

¹⁶J. O. Lee, G. Lientschnig, F. Wiertz, M. Struijk, R. A. J. Janssen, R. Egberink, D. N. Reinhoudt, P. Hadley, and C. Dekker, *Nano Lett.* **3**, 113 (2003).

¹⁷Y. N. Xia and G. M. Whitesides, *Annu. Rev. Mater. Sci.* **28**, 153 (1998).

¹⁸Y. L. Loo, D. V. Lang, J. A. Rogers, and J. W. P. Hsu, *Nano Lett.* **3**, 913 (2003).

¹⁹K. T. Shimizu, J. D. Tabbri, J. J. Jelincic, and N. A. Melosh, *Adv. Mater. (Weinheim, Ger.)* **18**, 1499 (2006).

²⁰A. Kumar and G. M. Whitesides, *Appl. Phys. Lett.* **63**, 2002 (1993).

²¹J. A. Rogers, Z. Bao, K. Baldwin, A. Dodabalapur, B. Crone, V. R. Raju, V. Kuck, H. Katz, K. Amundson, J. Ewing, and P. Drzaic, *Proc. Natl. Acad. Sci. U.S.A.* **98**, 4835 (2001).

²²N. B. Zhitenev, A. Erbe, Z. A. Bao, W. R. Jiang, and E. Garfunkel, *Nanotechnology* **16**, 495 (2005).

²³N. B. Zhitenev, A. Erbe, and Z. Bao, *Phys. Rev. Lett.* **92**, 186805 (2004).

²⁴X. Fan, D. T. Tran, D. P. Brennan, and S. R. J. Oliver, *J. Phys. Chem. B* **110**, 11986 (2006).

²⁵A. N. Caruso, L. G. Wang, S. S. Jaswal, E. Y. Tsybal, and P. A. Dowben, *J. Mater. Sci.* **41**, 6198 (2006).

²⁶D. K. Sarkar, M. Falke, H. Giesler, S. Teichert, G. Beddies, and H. J. Hinneberg, *J. Appl. Phys.* **89**, 6506 (2001).

²⁷G. E. Poirier, *Chem. Rev. (Washington, D.C.)* **97**, 1117 (1997).

²⁸N. Bowden, S. Brittain, A. G. Evans, J. W. Hutchinson, and G. M. Whitesides, *Nature (London)* **393**, 146 (1998).

²⁹N. B. Zhitenev, W. R. Jiang, A. Erbe, Z. Bao, E. Garfunkel, D. M. Tennant, and R. A. Cirelli, *Nanotechnology* **17**, 1272 (2006).

³⁰M. L. Chabinyc, X. X. Chen, R. E. Holmlin, H. Jacobs, H. Skulason, C. D. Frisbie, V. Mujica, M. A. Ratner, M. A. Rampi, and G. M. Whitesides, *J. Am. Chem. Soc.* **124**, 11730 (2002).

³¹A. S. Blum, J. G. Kushmerick, S. K. Pollack, J. C. Yang, M. Moore, J. Naciri, R. Shashidhar, and B. R. Ratna, *J. Phys. Chem. B* **108**, 18124 (2004).

³²J. G. Kushmerick, D. B. Holt, J. C. Yang, J. Naciri, M. H. Moore, and R. Shashidhar, *Phys. Rev. Lett.* **89**, 086802 (2002).

³³C. A. Richter, D. R. Stewart, D. A. A. Ohlberg, and R. S. Williams, *Appl. Phys. A: Mater. Sci. Process.* **80**, 1355 (2005).

³⁴C. A. Hacker, P. Liu, D. J. Vanderah, C. A. Richter, and L. J. Richter, *Abstr. Pap. - Am. Chem. Soc.* **230**, U1057 (2005).

³⁵W. R. McGovern, F. Anariba, and R. L. McCreery, *J. Electrochem. Soc.* **152**, E176 (2005).